PROCEDURES FOR EXPERIMENTAL MEASUREMENT AND THEORETICAL ANALYSIS OF LARGE PLASTIC DEFORMATIONS

by Richard E. Morris

Lewis Research Center

Cleveland, Ohio 44135

1. Report No. NASA TM X-3027	2. Government Accession No.	3. Recipient's Catalog No.
4. Title and Subtitle PROCEDURES FOR EXPERIMENTAL MEASUREMENT AND THEORETICAL ANALYSIS OF LARGE PLASTIC DEFORMATIONS		5. Report Date JUNE 1974
		6. Performing Organization Code
7. Author(s) Richard E. Morris		8. Performing Organization Report No. E-7661
9. Performing Organization Name and Address Lewis Research Center National Aeronautics and Space Administration Cleveland, Ohio 44135		10. Work Unit No. 770-18
		11. Contract or Grant No.
		13. Type of Report and Period Covered Technical Memorandum
12. Sponsoring Agency Name and Address National Aeronautics and Space Administration Washington, D.C. 20546		
		14. Sponsoring Agency Code

15. Supplementary Notes

16. Abstract

Theoretical equations are derived and analytical procedures are presented for the interpretation of experimental measurements of large plastic strains in the surface of a plate. Orthogonal gage lengths established on the metal surface are measured before and after deformation. The change in orthogonality after deformation is also measured. Equations yield the principal strains, deviatoric stresses in the absence of surface friction forces, true stresses if the stress normal to the surface is known, and the orientation angle between the deformed gage line and the principal stress-strain axes. Errors in the measurement of nominal strains greater than 3 percent are within engineering accuracy. Applications suggested for this strain measurement system include the large-strain - stress analysis of impact test models, burst tests of spherical or cylindrical pressure vessels, and to augment small-strain instrumentation tests where large strains are anticipated.

17. Key Words (Suggested by Author(s)) Structural mechanics	18. Distribution Statement Unclassified - unlimited Category 32		
19. Security Classif. (of this report) Unclassified	20. Security Classif. (of this page) Unclassified	21. No. of Pages 33	22. Price* $3.25

PROCEDURES FOR EXPERIMENTAL MEASUREMENT AND THEORETICAL

ANALYSIS OF LARGE PLASTIC DEFORMATIONS

by Richard E. Morris

Lewis Research Center

SUMMARY

Large plastic strains were generated in spherical model containment
vessels tested in impact against reinforced concrete blocks. Strains were
calculated from measurements of the change in length of orthogonal pairs of
lines established on the surface of a spherical model. Methods were avail-
able for interpreting strains when the gage lines were parallel or perpen-
dicular to lines of symmetry on the deformed model. However, some method
was needed for interpreting strain measurements on gage lines randomly
oriented in a field of uniform strain.

Equations are derived and analytical procedures are presented for in-
terpreting experimental measurements of large plastic strains by using or-
thogonal gage lines established on the surface of a plate so that the orien-
tation angle between a gage line and a principal strain axis is random.
Gage lines are measured before and after deformation. The change in orthog-
onality is also measured. Equations are solved to obtain the orthogonal
principal strains and to locate the direction of the principal strain axes
with respect to the deformed gage lines. When the stress normal to the sur-
face is nonzero and unknown, deviatoric stresses can be found but the true
stresses cannot be determined. When the stress normal to the surface is
zero or known, the principal stresses associated with the deformation can be
calculated.

The total error in strain measurement at the 1 percent strain level is
25 percent. Accuracy increases rapidly as the level of strain increases.
For nominal strains of 3 percent or more, the total error in strain measure-
ment is within the range of engineering accuracy.

The strain measurement system presented is particularly applicable to
the stress analysis of model containment vessels tested in impact against
reinforced concrete blocks. Other applications suggested include burst
tests of spherical or cylindrical pressure vessels and the augmentation of
small-strain instrumentation to provide data on large strains generated be-
yond the range of the small-strain instruments.

INTRODUCTION

Containment vessels are designed to contain radioactive materials such as nuclear reactors, nuclear fuels, isotopes, or nuclear waste products. The integrity of the vessel must be maintained even after severe deformation resulting from an accident. Stationary containment vessels may be subject to impact damage caused by objects in motion, for example, a falling aircraft. Mobile containment vessels may be damaged during an impact, such as in a collision or derailment of a train.

Nuclear reactors generate radioactive waste materials that must be collected and stored. Waste contained in spent fuel must be shipped from the reactor site to the reprocessing plant. Separated waste must then be moved from the reprocessing plant to a storage location. Radioactive materials being transported must be safely contained, even in the event of a catastrophic accident, to prevent contamination of the environment. One method of containing them is to enclose the radioactive materials in a spherical containment vessel which is capable of surviving a high-velocity accident.

The author's previous work (ref. 1) indicated that spherical containment vessels could survive high-velocity impacts. A testing program was initiated to obtain experimental data on the survivability of model vessels tested by impact against reinforced concrete blocks. Although models survived the high-velocity impacts, they were severely deformed. One measure of the severity of the deformation is to measure the plastic strain in the vessel wall and then compare that with the ultimate strain obtained from dynamic tensile tests of specimens machined from model material. If the total strain in the deformed model approaches the ultimate strain for the shell material, failure of the shell could result. Failure of the shell would result in the release of the radioactive contents of the containment vessel. The safety of the population and the environment requires that this condition must be avoided.

Impact forces between a model and a reinforced concrete block that equal as much as 30 000 times the force of gravity have been observed in a test (ref. 2). None of the many strain measurement instruments available could survive the tremendous impact forces to provide data on the large plastic strains generated in the shell of the model during impact.

An experimental method of strain measurement (ref.3) was devised that involved establishing gage lines on the surface of the model. Orientation of the model and target were controlled so that gage lines were parallel and perpendicular to lines of symmetry on the model before and after the impact test. Physical measurement of the change in length of gage lines provided principal nominal strain data that could be analyzed to obtain the maximum level of plastic strain in the model.

Control of the orientation of the model during impact was lost when test procedures were changed to obtain higher velocity impacts. Strain data were generated on deformed models that could not be analyzed because the gage lines were not parallel to principal strain axes and thus the experimental strain measurements were not principal strains. A method was needed for the analysis of randomly oriented strain measurements to obtain the direction and magnitudes of the principal plastic strains.

Analyses of finite strains contained in the literature on plasticity were not applicable to the measurement of large deformations. The procedures for the experimental measurement and analysis of large plastic strains and stresses presented herein were developed to solve this problem of strain interpretation.

The measurements made in this study and used in the analysis were in the U.S. customary system of units. Conversion to the International System of Units (SI) was done for reporting purposes only.

SYMBOLS

E   principal nominal plastic strain, cm/cm

EE $\Delta L/L$ on gage line, nominal apparent plastic strain, cm/cm

G   rise-gage length, cm

K   strength coefficient, N/cm^2

L   gage-line surface length, cm

$\bar{L}$ gage-line vector, cm

L'   gage-line surface length after deformation, cm

$\bar{L}'$ deformed gage-line vector, cm

n   strain-hardening exponent

R   surface radius, cm

X   chord length of a gage line, cm

Y   rise measurement, cm

β gage-line strain ratio, $(1 + EE_2)/(1 + EE_1)$

γ total shear angle, rad

γ_1 shear angle adjacent to E_1 principal axis, rad

γ_2 shear angle adjacent to E_2 principal axis, rad

ε true strain, $\ln(1 + E)$, cm/cm

ε_0 equivalent strain by distortion energy theory, cm/cm

η principal strain ratio, $(1 + E_2)/(1 + E_1)$

θ angle between gage line and principal axis, rad

σ true stress, N/cm²

σ' deviatoric stress, N/cm²

σ_0 equivalent stress by distortion energy theory, N/cm²

Subscripts:

m   mean

o   equivalent

ANALYSIS

The following assumptions were applied in the analysis of large plastic strains in surfaces of plates:

(1) The material is isotropic.
(2) Elastic strains are neglected.
(3) The state of plastic strain is constant throughout the element.
(4) Orthogonal principal axes of stress and plastic strain coincide.
(5) One principal axis of the orthogonal set of stress-strain axes is normal to the surface of the element during deformation.

(6) A gage line established on a metal surface has a uniform radius before deformation. Although changed during deformation, the radius of the gage line is assumed to be uniform after plastic deformation.

(7) Plastic strains are proportional to and have directions parallel to the lines of action of the stresses acting.

(8) Parallel lines are parallel before and after straining.

(9) Plastic strains result from monotonically increasing or decreasing equivalent stress.

(10) Equivalent stress and strain associated with plastic flow in the element are given by the distortion energy theory.

Most of the assumptions are common assumptions in plasticity. Assumption 5 is made to avoid surfaces loaded with friction forces which cause rotation of the stress axis away from the surface normal. Assumption 6 is needed for use in simplifying the measurement of the radii of the metal surface. Assumption 9 eliminates stress calculation in locations where stresses and strains undergo a reversal of sign. In such locations the final level of strain can be measured, but the final stress system cannot be obtained. Thus, the assumptions delineated provide limitations for the application of this system of plastic strain measurement and analysis.

The procedure for the analysis involves presenting the geometry for the strain measurement problem and solving geometric and vector equations to obtain data on the principal nominal strains and stresses associated with the large plastic deformations.

Figure 1(a) shows a random element on a metal surface. Two perpendicular gage lines are scribed on the surface of the element. In the figure, gage line $\overline{OA}$ is perpendicular to $\overline{OE}$. Gage line $\overline{OA}$ makes an angle θ with the X-axis, a principal stress-strain axis. Figure 1(b) shows the same element after orthogonal stresses σ_1 and σ_2 have plastically deformed the element. The stresses are parallel to the X-Y axes as shown. The stresses cause uniform nominal principal plastic strains E_1 parallel to the X-axis and E_2 parallel to the Y-axis. Erecting $\overline{OC}$ perpendicular to $\overline{OA'}$ forms the angle B'OC. This is the shear angle γ.

Physical measurements obtainable from the random element before and after impact are the change in length of $\overline{OA}$ and $\overline{OB}$ and the shear angle γ. The principal stresses and strains remain parallel and orthogonal, but the gage lines $\overline{OA}$ and $\overline{OB}$ rotate with respect to the principal X-Y axes.

5

Consequently, the change in the lengths of the gage lines cannot be direct-
ly interpreted as nominal strain in the random plate element. Relations
will be developed between the changes in the lengths of gage lines and the
shear angle so that the principal stresses and strains and the orientation
of the principal strain axes in the plastically deformed element can be
calculated.

Consider the case where the nominal principal plastic strain E_2 is
greater than E_1. Referring to figure 2, let $\overline{OA} = \overline{OB} = L$, the initial
length of a gage line. Denote the coordinates of point A by (x_1, y_1)
and point B by (x_2, y_2). The figure shows the gage lines before and
after plastic deformation. Primes denote the gage line and the
coordinates after straining.

According to assumption 3, each unit element in the plate parallel to
one of the principal strain axes undergoes a uniform plastic strain. The
principal strain parallel to the X-axis is denoted by E_1. Thus, the
element of length x_1 from point A perpendicular to the Y-axis is
strained uniformly with the nominal principal plastic strain E_1. The
change in the length of the element is $E_1 x_1$, as shown in figure 2.
Similarly, the element of length Y_1 from point A perpendicular to the
X-axis is strained with the nominal principal plastic strain E_2. The
change in length is $E_2 y_1$.

As plastic deformation takes place, point A moves to position A´
relative to the center of the coordinate system at point O. As gage line
$\overline{OA}$ is rotated during deformation to position $\overline{OA´}$, the shear angle γ_1
is formed. Determination of the angle $\theta + \gamma_1$ will make it possible to
locate the principal plastic strain axis E_1 on the deformed surface. In
a similar manner, point B moves to B´ and shear angle γ_2 is formed.
Since, in general, γ_1 is not equal to γ_2, only the sum of the angles γ
can be measured experimentally.

Relations between the experimental variables and the shear angles can
be simply obtained by using vector equations. The undeformed and the plas-
tically deformed gage lines are expressed as vectors. Unit vectors i
and j are parallel to the x- and y-axes, respectively.

$$\overline{L}_1 = L_1 \cos \theta i + L_1 \sin \theta j \tag{1a}$$

$$\overline{L}_1´ = L_1 \cos \theta (1 + E_1) i + L_1 \sin \theta (1 + E_2) j \tag{1b}$$

$$\overline{L}_2 = -L_2 \sin \theta i + L_2 \cos \theta j \tag{1c}$$

$$\bar{L}'_2 = -L_2 \sin \theta (1 + E_1) i + L_2 \cos \theta (1 + E_2) j \qquad (1d)$$

Calculations are simplified by using the experimental nominal apparent strain ratio β.

$$\beta = \frac{1 + EE_2}{1 + EE_1} \qquad (2)$$

In this ratio, EE_1 is the nominal apparent plastic strain on gage-line L_1 and EE_2 is the corresponding strain on gage-line L_2. Ratios of final gage-line length to initial gage-line length are used to evaluate β.

$$1 + EE_1 = \frac{\sqrt{(\bar{L}'_1)^2}}{\sqrt{(\bar{L}_1)^2}}$$

$$1 + EE_2 = \frac{\sqrt{(\bar{L}'_2)^2}}{\sqrt{(\bar{L}_2)^2}}$$

The symbol η is used to simplify the nominal principal plastic strain relations in the calculations.

$$\eta = \frac{1 + E_2}{1 + E_1} \qquad (3)$$

Using the definition of the ratio η and substituting in the vector equations (1) yield

$$1 + EE_1 = (1 + E_1) \cos \theta \sqrt{1 + \eta^2 \tan^2\theta} \qquad (4a)$$

$$1 + EE_2 = (1 + E_1) \cos \theta \sqrt{\eta^2 + \tan^2\theta} \qquad (4b)$$

The ratio β is obtained from equations (4).

$$\beta = \sqrt{\frac{\tan^2\theta + \eta^2}{1 + \eta^2 \tan^2\theta}} \tag{5a}$$

In the experimental plastic strain measurement problem, the ratio η is not known. Equation (5a) can be solved for η.

$$\eta = \sqrt{\frac{\tan^2\theta - \beta^2}{\beta^2 \tan^2\theta - 1}} \tag{5b}$$

The minus signs are omitted from equations (5a) and (5b) since neither of the ratios can be negative.

A relation for the total shear angle γ is found by using the vector equation

$$\cos\left(\frac{\pi}{2} - \gamma\right) = \sin\gamma = \frac{\overline{L}_1' \cdot \overline{L}_2'}{\sqrt{(\overline{L}_1')^2 (\overline{L}_2')^2}}$$

Substituting from equations (1) and simplifying yields

$$\sin\gamma = \frac{(\eta^2 - 1)\sin\theta\cos\theta}{\{(\eta^2\sin^2\theta + \cos^2\theta)(\sin^2\theta + \eta^2\cos^2\theta)\}^{1/2}}$$

This relation can be simplified by using the trigonometric identity for $\sin 2\theta$

$$\sin\gamma = \frac{(\eta^2 - 1)\sin 2\theta}{\left\{4\left[\eta^2\sin^4\theta + \eta^2\cos^4\theta + (\eta^4 + 1)\frac{\sin^2 2\theta}{4}\right]\right\}^{1/2}}$$

Simplification of the denominator yields

$$\sin\gamma = \frac{(\eta^2 - 1)\sin 2\theta}{[4\eta^2 + (\eta^2 - 1)^2\sin^2 2\theta]^{1/2}} \tag{6a}$$

A right triangle can be labeled by using equation (6a) to obtain other functions of the shear angle, as shown in figure 3. Tan γ is obtained from figure 3.

$$\tan' \gamma = \frac{(\eta^2 - 1)\sin 2\theta}{2\eta} \qquad (6b)$$

The equation can then be solved for $\eta = f(\theta, \gamma)$.

$$\eta^2 \sin 2\theta - 2\eta \tan \gamma - \sin 2\theta = 0$$

$$\eta = \frac{\tan \gamma}{\sin 2\theta} + \sqrt{\left[\frac{\tan \gamma}{\sin 2\theta}\right]^2 + 1} \qquad (7)$$

The minus sign is omitted on the radical since η cannot be negative.

The angle γ_1 between the two vectors $\overline{L}_1$ and $\overline{L}_1'$ can be found from the vector equation

$$\cos \gamma_1 = \frac{\overline{L}_1 \cdot \overline{L}_1'}{\sqrt{(\overline{L}_1)^2 (\overline{L}_1')^2}}$$

After substitution and simplification with the aid of trigonometric identities, a relation for $\tan \gamma_1$ is found.

$$\tan \gamma_1 = \frac{(\eta - 1)\tan \theta}{1 + \eta \tan^2 \theta} \qquad (8)$$

In a like manner when vector equations for L_2 and L_2' are used, the equation for $\tan \gamma_2$ is obtained.

$$\tan \gamma_2 = \frac{(\eta - 1)\tan \theta}{\eta + \tan^2 \theta} \qquad (9)$$

Equations (8) and (9) indicate that, in general, γ_1 is not equal to γ_2. Setting the partial differentials of γ_1 and γ_2 with respect to θ equal to 0 gives the location of the maxima.

$$\frac{\partial \gamma_1}{\partial \theta} = 0 \qquad \text{where } (\gamma_1)_{max} \text{ at } \theta = \tan^{-1} \eta^{-1/2} \qquad (10)$$

9

$$\frac{\partial \gamma_2}{\partial \theta} = 0 \qquad \text{where } (\gamma_2)_{max} \text{ at } \theta = \tan^{-1} \eta^{1/2} \qquad (11)$$

Substitution of values of θ for maximum shear angles into equations (8) and (9) reveals that the maximum shear angles are equal although the maximum values occur at different angles of orientation with respect to the principal axes of plastic strain.

$$(\gamma_1)_{max} = (\gamma_2)_{max} = \tan^{-1}\left[\frac{1}{2}(\eta^{1/2} - \eta^{-1/2})\right] \qquad (12)$$

A solution for angle θ in terms of the experimental variables β and γ is needed to determine the orientation of the gage lines with respect to the principal plastic strain axes. The relation required is obtained by eliminating η from equations (5b) and (7)

$$\eta = \sqrt{\frac{\tan^2\theta - \beta^2}{\beta^2 \tan^2\theta - 1}} \qquad (5b)$$

$$\eta = \frac{\tan \gamma}{\sin 2\theta} + \sqrt{\frac{\tan^2\gamma}{\sin^2 2\theta} + 1} \qquad (7)$$

Let

$$A = \frac{\tan \gamma}{\sin 2\theta}$$

$$C = \frac{\tan^2\theta - \beta^2}{\beta^2 \tan^2\theta - 1}$$

Substituting A and C into equations (5b) and (7) and squaring to eliminate the radicals lead to

$$C + \frac{1}{C} = 2(2A^2 + 1)$$

Then let

10

$$x = \sin 2\theta$$

$$y = 1 + \cos 2\theta$$

Replace the values for A and C in the equation and substitute x and y for trigonometric functions of θ. Note that

$$\frac{x}{y} = \tan \theta$$

$$x^2 + y^2 = 2y$$

$$\frac{x^2 - \beta^2 y^2}{\beta^2 x^2 - y^2} + \frac{\beta^2 x^2 - y^2}{x^2 - \beta^2 y^2} = \frac{4 \tan^2 \gamma}{x^2} + 2$$

The y term drops out upon simplification and results in an equation for x^2.

$$x^2 = \frac{4\beta^2 \tan^2 \gamma}{(\beta^2 - 1)^2 + (\beta^2 + 1)\tan^2 \gamma}$$

Substituting for x and simplifying results in

$$\sin 2\theta = \frac{2\beta \sin \gamma}{\sqrt{(\beta^2 - 1)^2 + 4\beta^2 \sin^2 \gamma}} \qquad (13)$$

Equation (13) can be represented by a right triangle with an acute angle of 2θ, as shown in figure 4. The figure provides a simple relation between the angle θ and the variables β and γ, the experimental measurements.

$$\tan 2\theta = \frac{2\beta \sin \gamma}{\beta^2 - 1} \qquad (14)$$

This equation gives the angle of orientation θ directly from the experimental measurements of the nominal plastic strain on two orthogonal gage lines and the shear angle measurement. Then equation (5b) or (7) gives the value of the ratio η.

The angle between the E_1 principal axis and gage line $\overline{OA'}$ in figure 2 is $\theta + \gamma_1$. From the figure

$$\tan(\theta + \gamma_1) = \frac{(1 + E_2)y_1}{(1 + E_1)x_1} = \eta \tan \theta \tag{15}$$

At point O in figure 2, the principal nominal strain normal to the surface AOB is E_3. The nominal change in length of a unit gage length normal to the surface of the deformed element with sides parallel to gage lines $\overline{OA'}$ and $\overline{OB'}$ is EE_3. Strains E_3 and EE_3 coincide and are therefore equal.

Volume is constant during plastic deformation. A unit cubic element with sides parallel to the principal strain axes has a volume equal to unity before and after deformation.

$$(1 + E_1)(1 + E_2)(1 + E_3) = 1 \tag{16}$$

Also a unit cubic element with sides parallel to the orthogonal strain gage lines has sides of a parallelepiped after deformation. Two sides of the deformed element are parallel to the plastically strained gage lines, and the third side is normal to the surface. Constant volume of a unit cubic element whose sides are not initially parallel to the principal strain axes may be stated

$$(1 + EE_1)(1 + EE_2)(1 + EE_3)\cos \gamma = 1 \tag{17}$$

Combining equations (16) and (17) and the definition of η yields a solution for the principal strain E_1.

$$E_1 = \sqrt{\frac{\cos \gamma}{\eta}(1 + EE_1)(1 + EE_2)} - 1 \tag{18}$$

From the definition of η, E_2 can be found. Then E_3 is found from equation (16). The true principal strains are obtained

$$\varepsilon_i = \ln(1 + E_i) \qquad i = 1,2,3 \tag{19}$$

Assumptions 3 and 8 require that two parallel lines of equal length

will be parallel and have the same strain after deformation. In figure 5, gage lines $\overline{AB}$ and $\overline{CD}$ are perpendicular and of equal length. Line $\overline{AB}$ will undergo the same deformation as if it were established in position $\overline{CE}$. The shear angle developed during deformation in angle ECD will be exactly the same as in angle AOD. The relations developed for gage lines such as $\overline{EC}$ and $\overline{CD}$ are therefore applicable to gage lines laid out as mutually perpendicular at the midpoints of the gage lines, such as $\overline{AB}$ and $\overline{CD}$. The average plastic strains measured on a pair of gage lines such as $\overline{AB}$ and $\overline{CD}$ would be more representative of the state of deformation in the element since the nominal strains are more closely average strains in a small element of surface area.

Flow equations are given by Faupel(ref. 4).

$$\varepsilon_i = \frac{\varepsilon_o}{\sigma_o}\left[\sigma_i - \frac{1}{2}(\sigma_j + \sigma_k)\right] \qquad \begin{matrix} i,j,k = 1,2,3 \\ i \neq j \neq k \end{matrix} \qquad (20)$$

In these equations, σ_o and ε_o refer to the equivalent stress and strain given by the distortion energy theory.

$$\sigma_o = \frac{1}{\sqrt{2}}\sqrt{(\sigma_1 - \sigma_2)^2 + (\sigma_2 - \sigma_3)^2 + (\sigma_3 - \sigma_1)^2} \qquad (21)$$

$$\varepsilon_o = \frac{\sqrt{2}}{3}\sqrt{(\varepsilon_1 - \varepsilon_2)^2 + (\varepsilon_2 - \varepsilon_3)^2 + (\varepsilon_3 - \varepsilon_1)^2} \qquad (22)$$

The true stress-strain diagram obtained experimentally for the material in the surface being measured is assumed to be linear in the plastic range on a log-log plot. The equation for the stress-strain diagram can be written in the form

$$\sigma_o = K\varepsilon_o^n \qquad (23)$$

In this equation, K is the strength coefficient and n is the strain-hardening exponent. The equivalent stress and plastic strain given by equations(21)and(22)are related by this equation. After the three principal true strains are known, the equivalent strain is determined from equation(22). Then the equivalent stress is found from equation (23).

Deviatoric stresses are stresses from which the hydrostatic components have been removed. Hydrostatic stresses have equal components in all directions. They do not contribute to distortion energy. Consequently, they do not cause plastic deformation. The sum of a set of deviatoric stresses is zero.

$$\sigma'_1 + \sigma'_2 + \sigma'_3 = 0 \qquad (24)$$

When the equation (24) is combined with equations (20), the resulting equations reflect assumption 7.

$$\sigma'_i = \frac{2}{3} \frac{\sigma_o}{\epsilon_o} \epsilon_i \qquad i = 1,2,3 \qquad (25)$$

In equation (25), the deviatoric stresses are directly proportional to the true plastic principal strains.

If the stress normal to the surface is zero or known, the true principal biaxial stresses in the surface of the model are obtainable. For $\sigma_3 = 0$, the true stresses become

$$\sigma_1 = \sigma'_1 - \sigma'_3 \qquad (26a)$$

$$\sigma_2 = \sigma'_2 - \sigma'_3 \qquad (26b)$$

$$\sigma_3 = \sigma'_3 - \sigma'_3 \equiv 0 \qquad (26c)$$

When σ_3 is some known value, the true principal stresses in the surface are obtained by adjusting each of the three principal true stresses obtained in equations (26) by the same hydrostatic component to give σ_3, the known value.

If the stress normal to the surface is nonzero and unknown, the true stress system is indeterminate. For each set of deviatoric stresses, there are an infinite number of sets of principal stresses. Each set has the same value of distortion energy, but sets have different values of the hydrostatic stress component.

14

The final level of strain can be determined in the presence of a strain reversal, but stresses cannot be calculated. Any set of principal strains can be related to a set of deviatoric stresses if there is no strain reversal. If the stress normal to the surface is zero or known, the principal stresses can be calculated, in addition to the deviatoric stresses.

PROCEDURE

Procedures are presented for establishing gage lengths on metal surfaces to obtain stress and plastic strain data. Punchmarks are used to establish the gage lengths. The chordal distance between gage marks is used with a radius measurement to obtain the surface length between gage marks before and after deformation. Two gage lines are established perpendicular to each other. The total shear angle is measured as the difference between the angle after deformation and the original right angle. Equations from the section ANALYSIS are used with the experimental data to calculate the nominal and the true principal plastic strains.

Two stress systems related to the measured strains are considered. The deviatoric principal stresses are determined. Then the principal stresses are found for the case where the radial stresses normal to the surface are zero.

Two perpendicular gage lines are shown in figure 5. Punchmarks are used to locate the extremities of the gage lines $\overline{AB}$ and $\overline{CD}$. Chord lengths between punchmarks are measured as indicated in figure 6 by using a micrometer caliper such as the one shown in figure 7. The instrument designed to measure the rise is also shown in figure 7. The instrument is set to zero on a surface plate. The arms of the rise gage contact the surface, establishing a chord length equal to the rise-gage length, as shown in figure 6. The rise is indicated on the dial indicator with the gage spanning each pair of punchmarks.

The gage lines are established accurately perpendicular to each other. As plastic strain occurs, the gage lines effectively rotate in the strain field. The change in the right angle γ between the gage lines is measured for use as the total shear angle in the strain calculations. The radius along each gage line is assumed to be uniform. The rise-gage length and the rise measurement determine the radius of the surface. Triangle AOB in figure 8 is used to solve for R as a function of

G   and   Y.

$$R \;=\; \frac{G^2}{8Y} + \frac{Y}{2} \tag{27}$$

The length of a gage line is determined by the chord length measured between punchmarks, indicated by   X   in figure 6, and the radius of the surface given by equation (27).

$$L \;=\; 2R \; \sin^{-1}\!\left(\frac{X}{2R}\right) \tag{28}$$

where   L   is the length of the gage line before deformation and   L´,. the length of the gage line after deformation, is given by equation (28) using R   and   X   measurements obtained from the deformed gage lines.   Then the nominal strain on the gage length is obtained from

$$EE_1 \;=\; \frac{L_1' - L_1}{L_1} \tag{29}$$

where EE_1 and EE_2 identify the nominal strains on two originally perpendicular gage lines and EE_3 identifies the nominal strain normal to the surface of the two perpendicular gage lines.   Measurement of the shear angle, the change in the right angle between two gage lines, completes the experimental measurements.

The experimental nominal strain ratio   β   is obtained from the definition, equation (2).

$$\beta \;=\; \frac{1 + EE_2}{1 + EE_1} \tag{2}$$

The original angle   θ   between gage line L_1 and a principal strain axis (fig.2) is a function of   β   and the shear angle measurement   γ.   The angle θ   is given by

$$\theta \;=\; \frac{1}{2} \tan^{-1}\!\left(\frac{2\beta \sin \gamma}{\beta^2 - 1}\right) \tag{14}$$

Then the principal strain ratio [eq.(3)] is obtained by using equation (5b).

$$\eta = \sqrt{\frac{\tan^2\theta - \beta^2}{\beta^2 \tan^2\theta - 1}} \qquad (5b)$$

The principal plastic strains are obtained with equations (18), (3), and (16).

$$E_1 = \left[\frac{\cos\gamma}{\eta}(1 + EE_1)(1 + EE_2)\right]^{1/2} - 1 \qquad (18)$$

$$E_2 = \eta(1 + E_1) - 1 \qquad (3)$$

$$E_3 = \frac{1}{(1 + E_1)(1 + E_2)} - 1 \qquad (16)$$

The angle between the deformed gage line L_1' and the principal strain axis E_1 is $\theta + \gamma_1$ (fig. 2). The angle is obtained by using equation (15).

$$\theta + \gamma_1 = \tan^{-1}(\eta \tan\theta) \qquad (15)$$

True principal plastic strains are found by substituting the nominal principal strain data into

$$\varepsilon_i = \ln(1 + E_i) \qquad i = 1,2,3 \qquad (19)$$

Then the equivalent true strain by the distortion energy theory is found from

$$\varepsilon_0 = \frac{\sqrt{2}}{3}\sqrt{(\varepsilon_1 - \varepsilon_2)^2 + (\varepsilon_2 - \varepsilon_3)^2 + (\varepsilon_3 - \varepsilon_1)^2} \qquad (22)$$

Dynamic true stress-strain properties of the model material are correlated with the exponential equation (23) to obtain values for the strength coefficient K and the strain-hardening exponent n. Equivalent stresses are then found from

$$\sigma_0 = K\varepsilon_0^n \qquad (23)$$

Deviatoric stresses can be obtained by using

$$\sigma_i^{'} = \frac{2}{3} \frac{\sigma_o}{\epsilon_o} \epsilon_i \qquad i = 1,2,3 \qquad (25)$$

Finally, if the stress normal to the surface is zero, the true principal biaxial stresses in the surface of the model are given by equations(26).

$$\sigma_i = \sigma_i^{'} - \sigma_3^{'} \qquad i = 1,2,3 \qquad (26)$$

RESULTS

Analytical equations and procedures are presented for use in the experimental measurement and analysis of large plastic strains on a metal surface. Two orthogonal gage lines of equal length are established on the unstrained metal surface. The gage lines may have a random orientation with respect to the principal axes of plastic strain.

At a free surface of a flat or curved metal structure, the stress may be zero or have some value normal to the surface in the absence of friction. Any such surface will have a principal stress axis normal to the surface. The other two principal axes of an orthogonal set will lie in the metal surface.

The change in length of the gage lines plus the change in the right angle between the gage lines are measured. Equations are developed to locate the principal axes of strain with respect to the deformed gage lines and to evaluate the principal strains in the surface of the metal.

Equations based on the distortion energy theory are used to obtain values for equivalent strains. Flow equations from plasticity are used, with the condition that the sum of the deviatoric stresses is zero, to obtain a proportionality between deviatoric stresses and the experimentally measured strains.

True stresses can be obtained if the stress normal to the surface is zero or known. If the stress normal to the surface is nonzero and unknown, the true stresses are indeterminate. If a strain reversal occurred, strains can be measured but the stresses cannot be calculated.

DISCUSSION

Experimental Data

The behavior of experimental strain data was investigated by plotting variations of the experimental variables in a constant field of plastic strain. The case selected for study was 50 percent nominal plastic strain in simple tension since the method was developed for the purpose of measuring large plastic strains. The nominal principal strains in the uniform strain field are

$$E_1 = -0.1835$$

$$E_2 = 0.500$$

$$E_3 = -0.1835$$

The nominal principal plastic strain ratio η is also constant.

$$\eta = \frac{1 + E_2}{1 + E_1} = 1.837$$

The angle of orientation θ was allowed to vary from 0° to 90° to study the variation of the experimental variables in the uniform strain field.

Equation (6b) was used to obtain data for the graph of γ as a function of θ shown in figure 9. The graph shows that the shear angle γ is zero when the gage lines are parallel to axes of principal strain. The angle γ increases almost linearly with θ to approximately 30°. The maximum value occurs at 45°. The maximum value of γ, 32.88°, constitutes a considerable distortion of the original right angle between the two gage lines.

Equations (8) and (9) provided data for the graphs of γ_1 and γ_2 shown in figure 10. The graphs show that the individual angles of rotation of the gage lines are zero when the gage lines are parallel to the principal strain axes. They are equal at an orientation angle of 45°. The maximum values and the orientation of the individual angles of rotation of the gage lines is a function only of the principal strain ratio η.

Equation (10) gives the orientation angle θ for the maximum value of γ_1, and equation (11) gives the orientation angle for γ_2. The maximum value, which is the same for both angles γ_1 and γ_2, is determined by equation (12). As shown by figures 9 and 10 the total shear angle γ is quite sensitive to the angle of orientation. For this case of 50 percent plastic tensile strain, the total shear angle γ is about equal to the orientation angle θ over the range from $0°$ to $30°$.

Data for the graphs of EE_1 and EE_2 shown in figure 11 were obtained by using equations (4a) and (4b). The apparent strain on a gage line varies with the orientation of the gage line in the plastic strain field. Principal nominal strains are equal to the nominal strains measured on gage lines have values in between the principal values of strains E_1 and E_2. When the orientation angle θ has a value of $45°$, the nominal plastic strains measured on gage lines are equal.

A graph of the experimental strain ratio β versus the orientation angle θ is shown in figure 12. Data for the graph were calculated with equation (5a). Again experimental strain ratios are equal to principal nominal plastic strain ratios when $\theta = 0$ and the gage lines are parallel to the axes of principal strain. The graph passes through a value of 1.0 at $\theta = 45°$. This reflects the fact that the nominal strains on the gage lines are equal at that orientation, as illustrated in figure 11.

As shown by equation (8), γ_1 is a function of the principal nominal strain ratio η and the orientation angle θ. The orientation angle for the gage line L_1' in the strained position and the E_1 principal strain axis is $\theta + \gamma_1$. This angle would be expected to be a function of the same two variables since it is different from γ_1 by the angle θ. Equation (15) is the required relation. Figure 13 shows the variation of $\theta + \gamma_1$ as a function of θ for the special case of 50 percent nominal plastic tensile strain.

The possibility of neglecting the shear angle γ and using two experimental strain measurements EE_1 and EE_2 as principal nominal strains to calculate a value for equivalent strain was investigated. The error involved in neglecting the shear angle was obtained by taking the difference between the calculated value of strain and the uniform equivalent strain of the 50 percent simple tensile strain field. Values of apparent equivalent strain are plotted against the angle θ in figure 14. Correct values of 0.403-cm/cm equivalent strain were obtained only at $0°$ and $90°$. The maximum error, -7.45 percent, occurred at $30°$ and $60°$.

The error at 45° was -7.0 percent. If all gage lines were within ±10° of alinement with the principal axes of strain, the maximum error in assuming that measured equivalent strain was the true equivalent strain would be -1.0 percent.

Accuracy

Sources of error in the measurement of permanent deformations include instrument errors and punchmark deformation. Other sources of error to be assessed in using this method of measurement include the effects of averaging strain on the gage length and the effect of variation of the radius over the gage length. The assumption that elastic strains may be neglected may incorporate error in the form of elastic strains associated with residual stresses.

Errors in measurement varied with the level of strain being measured. Strains less than 0.1 percent could not be detected. Accuracy of measurement increased as the level of strain being measured increased. Two experimental measurements are required to determine the length of a gage line on a curved surface before deformation. Two more measurements are needed to obtain the deformed length. Measurement of the angle between two gage lines is a source of error. Errors were analyzed for three levels of strain: 1, 10, and 50 percent. The total error in strain measurement is the sum of the errors in the pretest and the post-test measurements. Results of the analysis are listed in table I.

The error analysis presumes that the pretest gage lengths are laid out and measured on a surface with a relatively uniform radius of 32 cm. Post-test error calculations are based on impact-deformed surface radii as short as 4.6 cm. All errors are based on gage lengths of 5.08 cm.

The error in a rise-gage reading was ±0.0013 cm when the jeweled dial indicator was read to the nearest whole division. The gage length of the rise gage shown in figure 7 is 3.175 cm. The rise-gage frame shown separately has a gage length of 6.350 cm. The large frame is used to measure surface radii greater than 10 cm. The smaller frame is used to measure radii less than 10 cm. All the pretest radius measurements were made with the 6.350-cm frame, and the apparent strain associated with the rise-gage reading error was small, as shown in table I. The effect of rise-gage error increased when the 3.175-cm frame was used to measure the

minimum radius on the deformed model. The maximum in this case was 5.6 percent error in the measurement of 1 percent strain.

The error in a dial caliper reading was ±0.0013 cm when the dial was read to the nearest division. This error caused an error of 2.5 percent in the measurement of 1 percent strain. Error decreased as the level of strain increased. This error component was the same for measurements before and after the test.

Deformation of the model affected the fit between the punchmarks and the points of the caliper. The centerline of a punchmark rotated when the surface radius changed. The shape of the conical punchmark surface was deformed by the plastic strain in the metal surface. This source of error was a maximum for the greatest change in radius during deformation of the model. This error increased as the level of strain increased, but the percent error was the same at all three levels of strain.

Applications

The strain measurement system is applicable to high-velocity impact since the gage lines established on the surface of a model do not contribute to inertia forces generated during impact. Strain gage lines have been established on the surfaces of 0.61-meter- (2.0-ft-) diameter model containment vessels tested under conditions of high-velocity impact against a reinforced concrete block. Extremities of gage lines were located by punchmarks. The strain measurement system survived the impact tests described in references 2 and 5.

As noted in the section ANALYSIS, the assumptions applied limit the application of this method of plastic strain measurement. Wherever the assumptions are in question, the use of this strain measurement method must also be questioned. The method cannot be used on a surface in the presence of surface friction forces. One of the principal stresses acts normal to a free surface. A friction force acts to change the direction of that principal stress so that it is not perpendicular to the surface, and thus assumption 5 does not hold. Stresses and strains are assumed to increase or decrease monotonically. This assumption eliminates the determination of principal stresses in surface locations where stresses and plastic strains undergo a reversal of sign. In such locations the strains can be measured, but the final stress system cannot be obtained.

The stress analysis of the hollow-sphere impact test reported in

reference 3 involved gage lines parallel and perpendicular to lines of symmetry on the model before and after deformation. Thus, the orthogonal gage lines were located parallel to the principal strain axes. The equations developed in the analysis section of this report are presented for use in the analysis of gage-line strain measurement data obtained from surfaces where the orthogonal gage lines may not be located parallel to the principal plastic strain axes.

This strain measurement system could be useful in tests of models or structures where the plastic strains are greater than the strain range measurement capability of available electronic or mechanical gages. Strains could be measured in cylinders tested under conditions of combined tension and torsion. Large creep deformation could be measured. Strains generated during burst tests of spheres and cylinders could be measured.

Strain gage lines may be located on surfaces by other methods to obtain lines capable of surviving other test conditions. For example, gage lines might be established by etching or scribing lines or points on surfaces of a model. Optical systems could be utilized to make possible the use of smaller gage lengths in order to increase the accuracy of measurement, or to obtain a more accurate measure of the average strain in the model in the presence of strain gradients.

This system of strain measurement could be used to augment other instrumentation sensitive to small strains since the system presented in this report cannot be used to measure small strains. The system can be used to obtain reliable measurements of large permanent deformations on metal surfaces wherever large strains are expected to occur.

The punchmarks defining two perpendicular gage lines were formed in the surface of the metal with a four-punch tool so that gage lines were accurately perpendicular before the test. After the test, angles were measured to the nearest 0.2° so that the error in the determination of the shear angle γ was ±0.1°. Figure 9 is a plot of the shear angle as a function of the angle of orientation in the strain field. The horizontal slope at θ = 45° corresponds with the gage-line orientation for the maximum error in strain measurement resulting from error in the shear angle measurement. As shown in table I, angle measurement error made the largest component of total error at the 1 percent strain level. Shear angle measurement error drops to 1 percent as the orientation angle goes to 0°. This source of error is less than 1 percent for measurments in a 15 percent strain area. The error decreases at higher levels of strain.

Total errors are the maximum errors that occur when all of the

component errors are maxima and act in the direction to increase the total error. Total errors are relatively large in areas of low strain. The error is within the range required for engineering accuracy of ±10 percent at higher levels of strain. Figure 15 shows that plastic strains above 3 percent have total errors in measurement of less than 10 percent.

In the usual case, some errors will be nonadditive or compensating so that the total error in a measurement will fall below the curve in figure 15. Error in the measurement of small strains can be reduced by keeping the orientation angle between a gage line and a principal strain axis as small as possible. Error contributions resulting from strain averaging over a gage length, variation of the radius on a gage length, or the presence of residual stresses and elastic strains must be evaluated for each measurement problem. Errors from these sources are in addition to the total error graphed in figure 15.

CONCLUDING REMARKS

Equations are derived and analytical procedures are presented for the experimental measurement of large plastic strains in the surface of a plate. Two perpendicular gage lines of equal length are established on the surface of the plate before deformation. The change in the lengths of the gage lines and the change in the right angle between the gage lines after deformation constitute the required experimental data.

Analysis of the data yields the principal plastic strains and the angle between an experimental gage line and a principal strain axis in the surface of the plate. True strains can be calculated and used to obtain equivalent strain. The behavior of the experimental variables was investigated by evaluating equations for the case of 50 percent permanent plastic deformation in simple tension.

Sources of error in strain measurement are discussed. It was shown that permanent plastic strains of 3 percent or more could be measured with engineering accuracy. Although the maximum error in the measurement of 1 percent strain is about 25 percent, the accuracy increases for larger strains. When the plastic deformation is the result of monotonically increasing strain, an orthogonal set of deviatoric stresses can be calculated. In addition, if the stress normal to the surface is

zero or known, the true stresses associated with the plastic deformation can be obtained.

Lewis Research Center,
    National Aeronautics and Space Administration,
        Cleveland, Ohio, November 19, 1973,
           770-18.

REFERENCES

1. Morris, Richard E.: Empirical Correlation of Small Hollow Sphere Impact Failure Data Using Dimensional Analysis. NASA TM X-52874, 1970.

2. Puthoff, R. L.; and Dallas, T.: Preliminary Results on 400 Ft/Sec Impact Tests of Two 2-Foot Diameter Containment Models for Mobile Nuclear Reactors. NASA TM X-52915, 1970.

3. Morris, R. E.: Experimental Stress Analysis of Plastic Deformations in a Hollow Sphere Deformed by Impact Against a Concrete Block. NASA TM X-68270, 1973.

4. Faupel, Joseph H.: Engineering Design, John Wiley & Sons, Inc., 1964.

5. Puthoff, Richard L.: A 1055 Ft/Sec Impact Test of a Two-Foot Diameter Model Nuclear Reactor Containment System Without Fracture. NASA TM X-68103, 1972.

TABLE I. - ERRORS IN PLASTIC STRAIN MEASUREMENT

Measurement	Level of plastic strain, percent		
	1	10	50
	Error, percent		
Pretest:			
Rise gage (R = 32.1 cm nominal)	0.2	0	0
Dial caliper	2.5	.3	.1
Post-Test:			
Rise gage (R ≤ 4.65 cm)	5.6	.6	.1
Dial caliper	2.5	.3	.1
Punchmark deformation	2.0	2.0	2.0
Shear angle (±0.1°)	11.8	1.3	.4
Total error, percent	24.6	4.5	2.7

(a) Before deformation.

(b) After deformation.
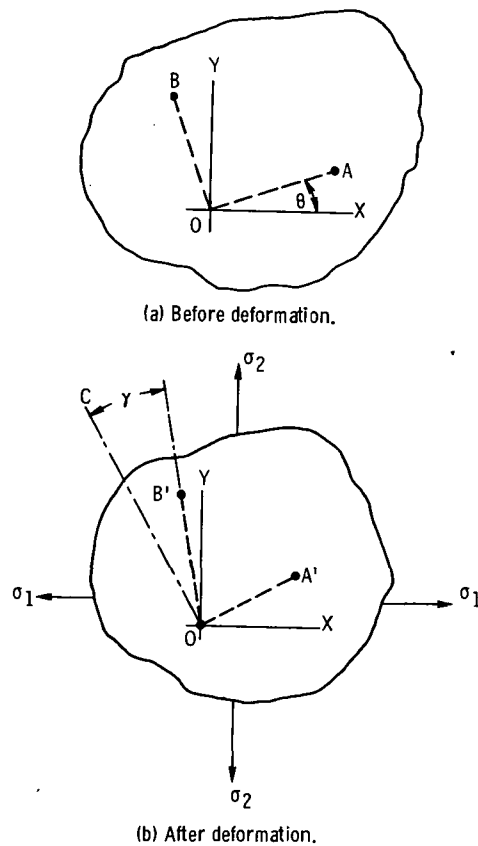
Figure 1. - Random plate element before and after uniform plastic deformation.
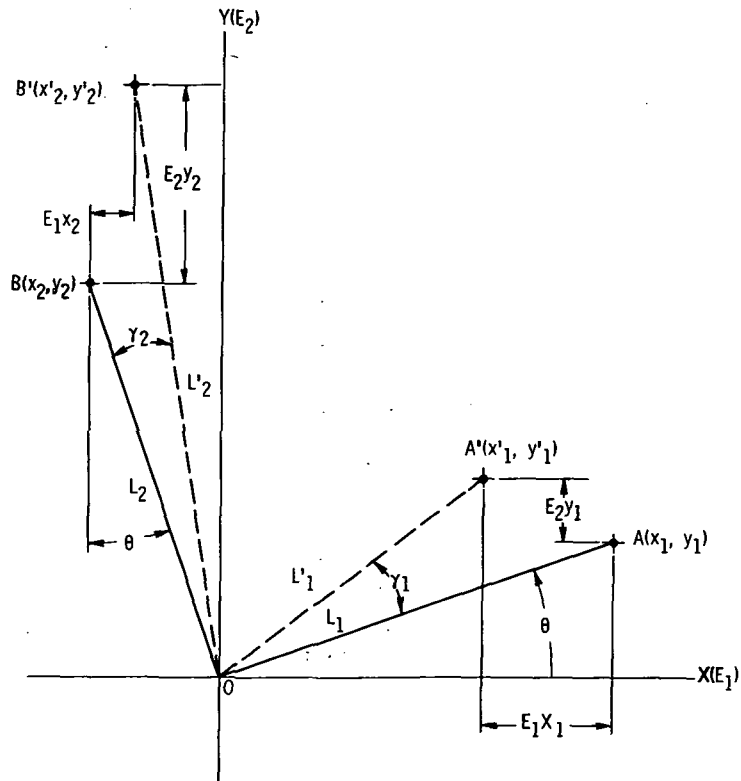
Figure 2. – Geometry of plastically strained gage lines.
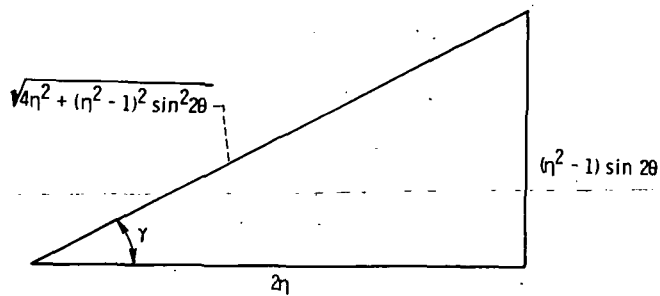
Figure 3. – Right triangle for angle γ.
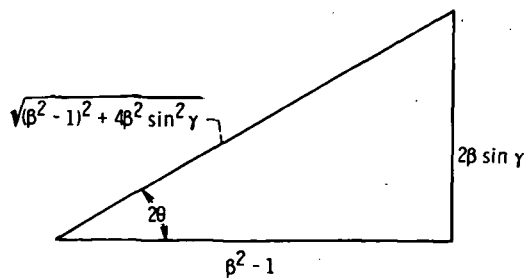
Figure 4. – Right triangle for angle 2θ from equations (6).
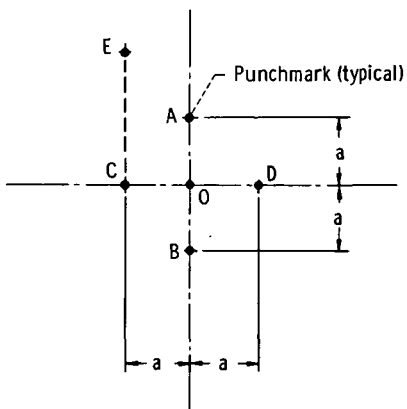
Figure 5. – Gage lines.
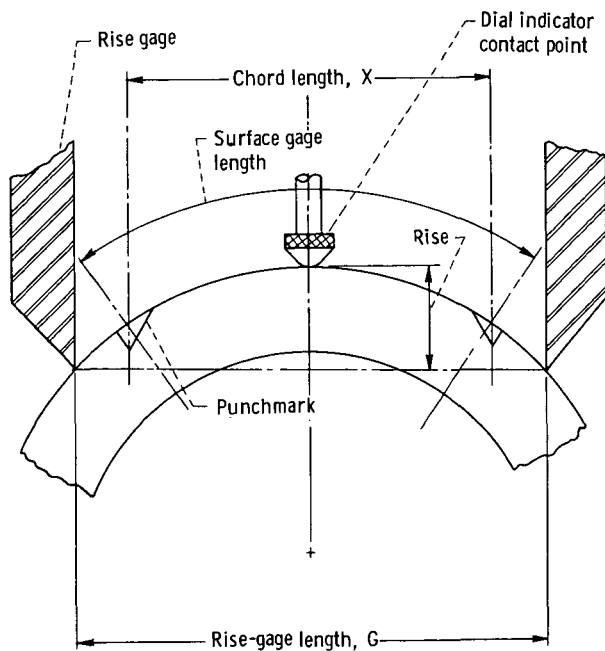
Figure 6. – Rise-gage measurement on a curved surface.
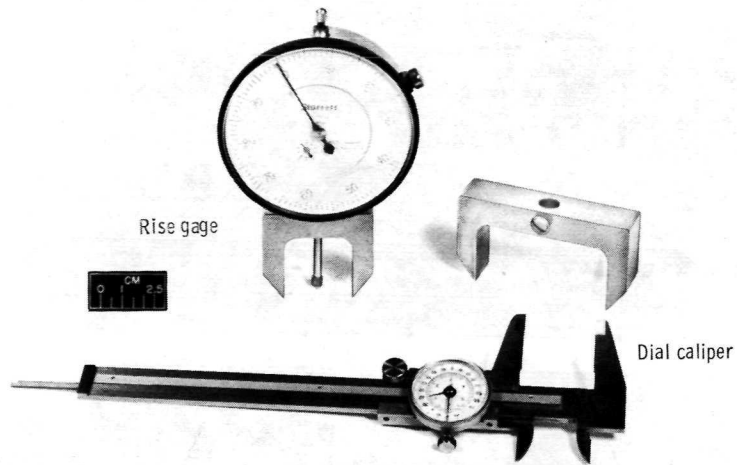
Figure 7. - Rise measurement gage with 3.175-cm (1.250-in.) gage
length, rise-gage frame with 6.350-cm (2.500-in.) gage length,
and dial caliper used for gage-line chord length measurement.
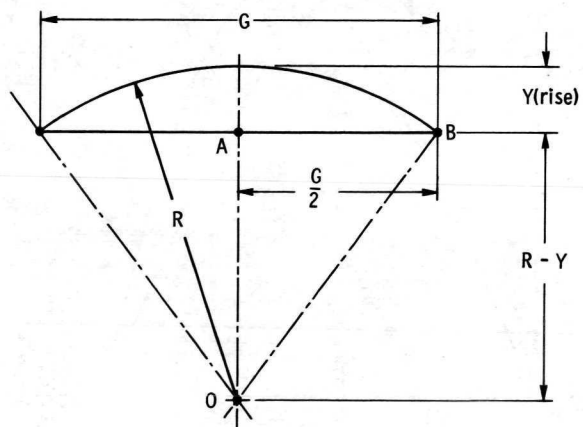
Figure 8. - Radius measurement using the rise gage.
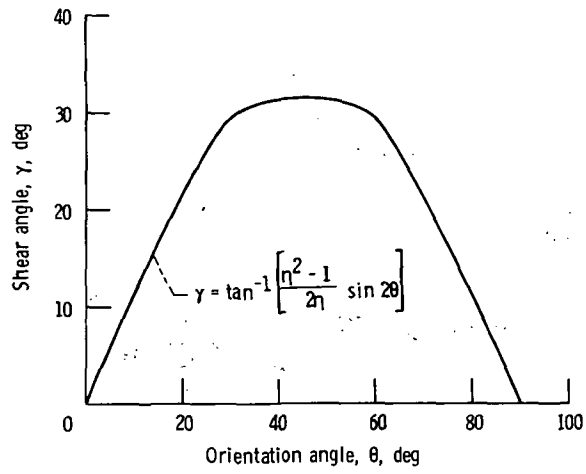
Figure 9. - Shear angle as function of orientation angle for 50 percent nominal plastic tensile strain.

$$\gamma = \tan^{-1}\left[\frac{\eta^2 - 1}{2\eta}\sin 2\theta\right]$$

$$\gamma_1 = \tan^{-1}\frac{(\eta - 1)\tan\theta}{1 + \eta\tan^2\theta}$$

$$\gamma_2 = \tan^{-1}\frac{(\eta - 1)\tan\theta}{\eta + \tan^2\theta}$$
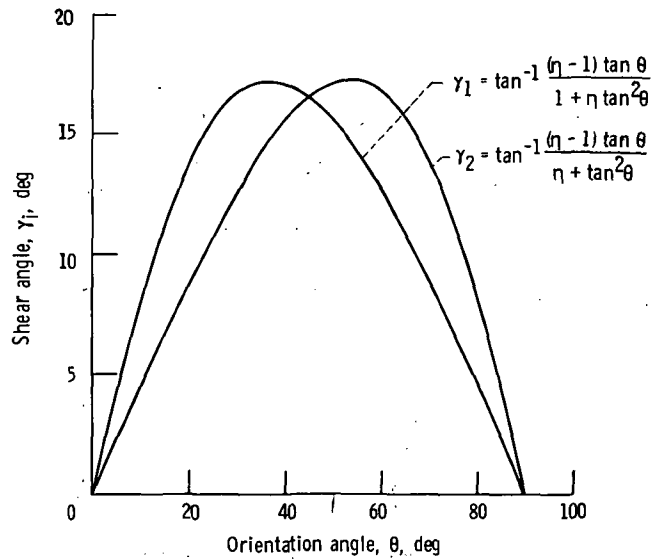
Figure 10. - Shear angles γ_1 and γ_2 as function of orientation angle for 50 percent nominal plastic tensile strain.
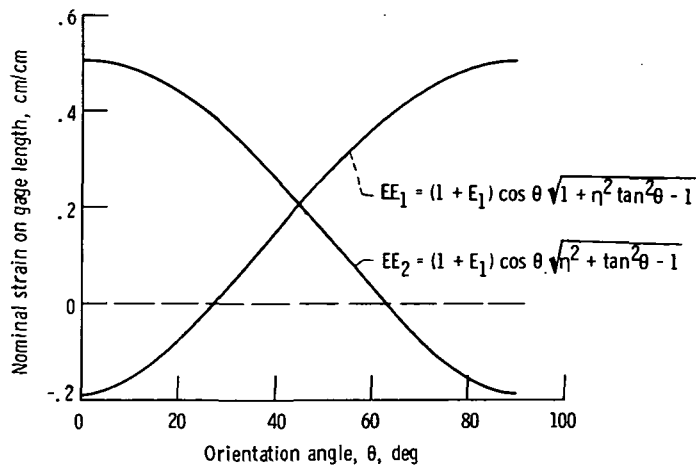
Figure 11. - Nominal apparent strain EE on two perpendicular gage lines as function of angle of orientation with a principal strain axis.

$$EE_1 = (1 + E_1) \cos \theta \sqrt{1 + \eta^2 \tan^2 \theta} - 1$$

$$EE_2 = (1 + E_1) \cos \theta \sqrt{\eta^2 + \tan^2 \theta} - 1$$

$$\beta = \sqrt{\frac{\tan^2 \theta + \eta^2}{1 + \eta^2 \tan^2 \theta}}$$
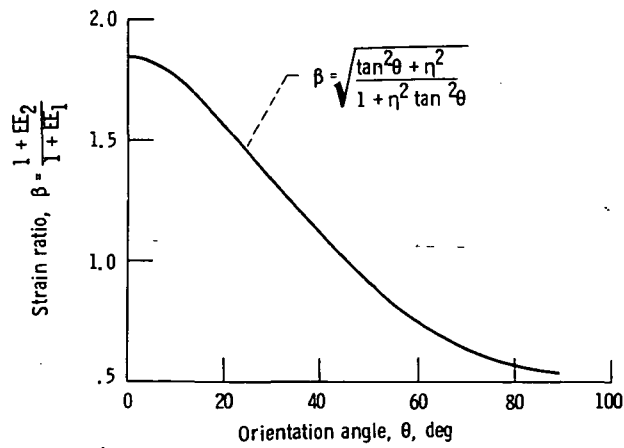
Figure 12. - Strain ratio as function of orientation angle for 50 percent nominal plastic tensile strain.
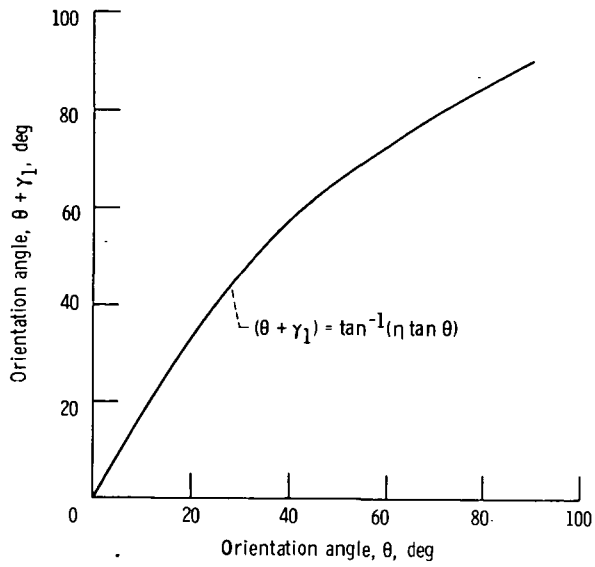
Figure 13. - Orientation angle $\theta + \gamma_1$ as function of orientation angle θ for 50 percent nominal plastic tensile strain.

$$(\theta + \gamma_1) = \tan^{-1}(\eta \tan \theta)$$
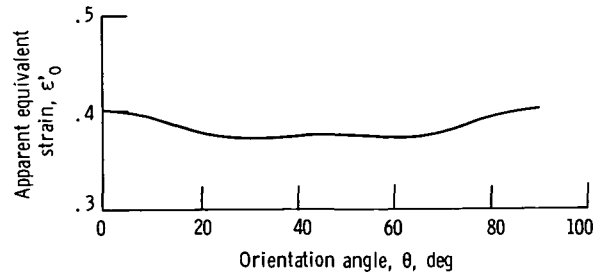
Figure 14. - Apparent strain as function of orientation angle, neglecting shear deformation and assuming that strains on two originally perpendicular gage lines are nominal principal plastic strains.
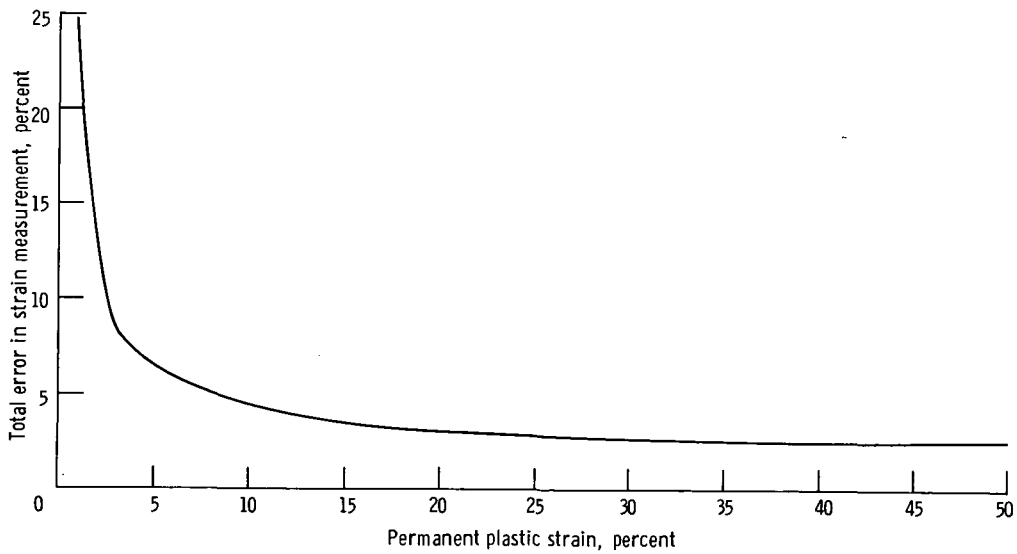
Figure 15. - Total error in experimental strain measurement as function of permanent plastic strain.

"The aeronautical and space activities of the United States shall be conducted so as to contribute . . . to the expansion of human knowledge of phenomena in the atmosphere and space. The Administration shall provide for the widest practicable and appropriate dissemination of information concerning its activities and the results thereof."
—NATIONAL AERONAUTICS AND SPACE ACT OF 1958

NASA SCIENTIFIC AND TECHNICAL PUBLICATIONS

TECHNICAL REPORTS: Scientific and technical information considered important, complete, and a lasting contribution to existing knowledge.

TECHNICAL NOTES: Information less broad in scope but nevertheless of importance as a contribution to existing knowledge.

TECHNICAL MEMORANDUMS: Information receiving limited distribution because of preliminary data, security classification, or other reasons. Also includes conference proceedings with either limited or unlimited distribution.

CONTRACTOR REPORTS: Scientific and technical information generated under a NASA contract or grant and considered an important contribution to existing knowledge.

TECHNICAL TRANSLATIONS: Information published in a foreign language considered to merit NASA distribution in English.

SPECIAL PUBLICATIONS: Information derived from or of value to NASA activities. Publications include final reports of major projects, monographs, data compilations, handbooks, sourcebooks, and special bibliographies.

TECHNOLOGY UTILIZATION PUBLICATIONS: Information on technology used by NASA that may be of particular interest in commercial and other non-aerospace applications. Publications include Tech Briefs, Technology Utilization Reports and Technology Surveys.

Details on the availability of these publications may be obtained from:

SCIENTIFIC AND TECHNICAL INFORMATION OFFICE

NATIONAL AERONAUTICS AND SPACE ADMINISTRATION
Washington, D.C. 20546